Key Engineering Materials
ISSN: 1662-9795, Vol. 987, pp 3-10
doi:10.4028/p-qO8WAd
© 2024 The Author(s). Published by Trans Tech Publications Ltd, Switzerland.
Submitted: 2023-11-18
Revised: 2024-03-02
Accepted: 2024-04-08
Online: 2024-09-23

Microstructure Evolution and FEM Prediction on AA6XXX Alloys

Marco Negozio[1,a*], Riccardo Pelaccia[2,b], Lorenzo Donati[1,c], Barbara Reggiani[2,d], Sara Di Donato[1,e]

[1]University of Bologna, DIN Department of Industrial Engineering, Viale Risorgimento 2, 40136, Bologna, Italy

[2]University of Modena and Reggio Emilia, DISMI Department of Sciences and Methods for Engineering, Via Amendola 2, 42122, Reggio Emilia, Italy

[a]marco.negozio2@unibo.it, [b]riccardo.pelaccia@unimore.it, [c]l.donati@unibo.it, [d]barbara.reggiani@unimore.it, [e]sara.didonato2@unibo.it

Keywords: recrystallization, aluminum alloy, FEM, extrusion, microstructure.

Abstract. The microstructure evolution during the extrusion process of AA6XXX aluminum alloys is getting a significant interest from extruders and researchers because of the effect of the grain structure on the extruded component properties. Several process and material parameters such as chemical composition, homogenization, temperature evolution, extrusion speed, geometries and quenching have a direct impact on the final grain size of extruded profiles. Because there are so many affecting elements, it is extremely challenging to forecast the microstructure evolution and, as a result, research activities are still required to understand and control the aluminum alloy recrystallization behaviour. In this work, a methodology for the microstructural characterization of AA6XXX aluminum alloys is proposed. The methodology involves the experimental investigation of the profile grain evolution during the extrusion process, the development of a AA6XXX recrystallization model optimized to describe the AA6063 recrystallization behaviour and the simulation by means of finite element method of the final microstructure of the extruded profile.

Introduction

Aluminum alloy extruded profiles have gained widespread prominence in contemporary engineering applications due to their combination of lightweight and mechanical strength [1-4]. The microstructure of these profiles, defined as the arrangement of crystals, grains, and phases at the microscopic level, plays a lead role in determining their mechanical properties, formability, corrosion resistance, and overall quality [5-7]. As the demand for high-performance materials continues to grow, understanding and optimizing the microstructure of aluminum alloys becomes mandatory to meet stringent engineering requirements.

In recent years, analytical recrystallization models have been developed as valuable tools for predicting dynamic and static recrystallization kinetics and, consequently, for estimating grain size evolution during and after the extrusion process. This study explores the feasibility of coupling recrystallization model with finite element simulations of the extrusion process. The primary focus is on characterizing the microstructural evolution of a AA6XXX aluminum alloys during extrusion, specifically in the case of a AA6063 hollow profile. A systematic methodology is proposed, which involves the collection of experimental data of grain size of a AA6063 extruded profile. This data is used to determine the material constants of the selected AA6XXX recrystallization model [8] and to optimize it for the specific alloy under investigation. Finally, this optimized AA6063 recrystallization model is implemented into the Qform Extrusion finite element code to simulate the final microstructure of the extruded profile.

Methodology

An optimized recrystallization model for the 6XXX aluminum alloy under consideration will be developed. The base recrystallization model for AA6XXX aluminum alloys, which enabled the prediction of statically and dynamically recrystallized grain size and recrystallization thickness

This article is an open access article under the terms and conditions of the Creative Commons Attribution (CC BY) license (https://creativecommons.org/licenses/by/4.0)

during hot forming procedures, was built on the work of Negozio et al. [8]. The relevant material constants are computed by compiling a group of numerical and experimental data gathered through relevant simulations and experiments. In detail, profiles are extruded using a range of process variables (such as varying ram speeds, billet pre-heating temperatures, etc.), and all the microstructural data is collected. In addition, the temperature, strain rate, and strain data must be extracted from the FEM simulations of the extrusion campaign. These data are merged with experimental one in order to calibrate the recrystallization model using a regression method. To forecast the microstructure following hot forming procedures, the investigated alloy recrystallization model is implemented in a post-processing subroutine to FEM simulations using Qform Extrusion software.

Experimental Investigation

The grain size data used for the calibration of the AA6063 recrystallization model was taken from the extrusion of a hollow profile analysed in Gamberoni et al. [9]. In Fig. 1, the microstructure of the investigated profile is shown. In order to acquire the image, the sample was cut in 6 parts: each one was grinded, polished, anodized (40 V dc, 4 min) with Barker's reagent (15 mL HBF4, 750 mL H2O) and then analysed using the optical microscopy Zeiss AXIO with polarized light. The profile was extruded using a 30 MN press at Sapa plant in Ornago (MI) and the sample was taken from the fifth billet of the extrusion cycle at the middle length of the extrusion profile.

The figure clearly depicts a fully recrystallized microstructure, with no evidence of fibrous grains and an average grain size ranging from 55 μm to 500 μm. A total of 100 points were randomly selected on the cross-section of the profile and analysed according to the ASTM E112 regulation. Half of these measurements were utilized to optimize the recrystallization model and determine the material constants for AA6063. This calibration process employed an optimization algorithm implemented in Matlab, as referenced in [8]. Subsequently, with the constants determined, the model was integrated into the post-processing subroutine of the FEM simulation. The remaining half of the measurements were then used to validate the model accuracy by comparing numerical predictions with the experimental grain size values.

All the process parameters and the geometries of the billet and tools are reported in Table 1.

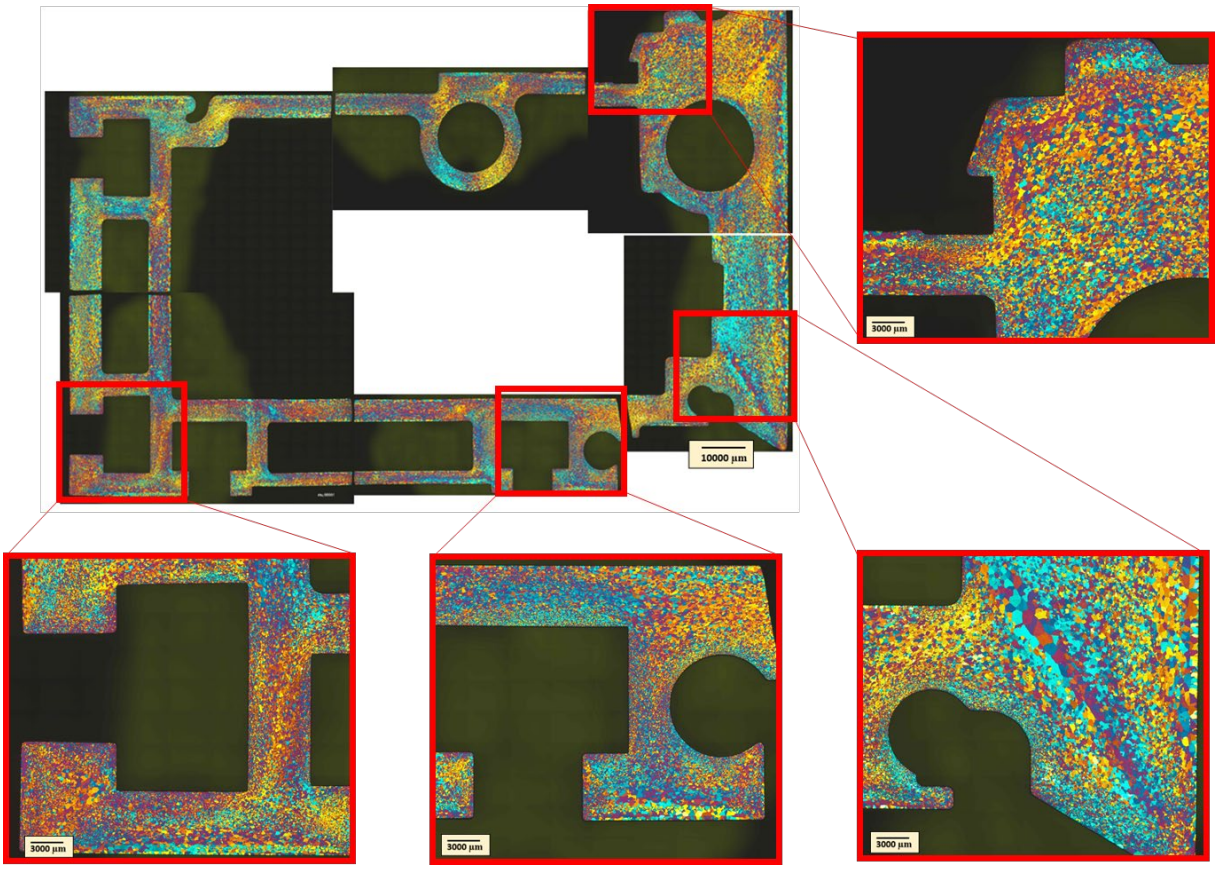

Fig. 1. Microstructure of the extruded AA6063 profile.

Table 1. Process parameters and workpiece/tools geometries.

Process parameters and geometry tolerances	Profile
Aluminum alloy	AA6063
Extrusion ratio	9.6
Ram speed [mm/s]	8.5
Container temperature [°C]	420
Billet temperature [°C]	470
Die temperature [°C]	450
Ram acceleration time [s]	5
Billet length [mm]	815
Ram stroke [mm]	765
Billet diameter [mm]	247
Container diameter [mm]	257
Billet Rest length [mm]	55
Billet grain size [µm]	135
Puller tensile force [N]	200

Hot torsion tests were performed in order to characterize the flow stress of the AA6063 billet material used for the extrusion of the profile under investigation [9]. A total of 12 conditions were tested, with temperatures of 450-500-550-575°C and strain rates of 0.01-1-10 s^{-1}. The data acquired were used to calibrate the Hensel-Spittel law [5] applied in the simulation of the extrusion process (Eq. 1).

$$\bar{\sigma} = A \cdot e^{m_1 T} \cdot \bar{\varepsilon}^{-m_2} \cdot \dot{\bar{\varepsilon}}^{-m_3} \cdot e^{\frac{m_4}{\bar{\varepsilon}}} \cdot (1+\bar{\varepsilon})^{m_5 T} \cdot e^{m_7 \bar{\varepsilon}} \cdot \dot{\bar{\varepsilon}}^{m_8 T} \cdot T^{m_9} \quad (1)$$

Table 2. Hensel-Spittel coefficients for the AA6063 aluminum alloy [9].

Parameters	AA6063
A	1014.7 [MPa]
m1	-0.00438 [K-1]
m2	0.2425
m3	-0.0965
m4	-0.000438
m5	-0.000766 [K-1]
m7	0.0939
m8	0.000291 [K-1]
m9	0

Modeling and Simulation

The recrystallization model used in the simulation was taken by the work of Negozio et al. [8]. The average grain diameter of the static recrystallized grain D_{rex} was calculated as follows:

$$D_{rex} = X_{rex} * N^{-1/3}, \quad (2)$$

where N is the nucleation density and X_{rex} is the fraction of recrystallized material. Since the obtained images demonstrate a totally recrystallized microstructure, the X_{rex} value was taken to be equal to 1. In order to determine N, different nucleation contributions must be considered [8]:

$$\mathrm{N} = N_{PSN} + N_{GB} + N_C. \quad (3)$$

The N_{PSN} is the nucleation from deformation zones around large particles, which involves the development of nuclei in high deformation zones with random orientations, is frequently the primary nucleation process in commercial alloys that contain large undeformable particles. Old grain boundaries, or N_{GB}, are the nucleation site for a random recrystallization texture. Around these deformation zones, randomly oriented subgrains can emerge. N_C is the nucleation from retained cube grains from the original material that endured the deformation [8].

These three nucleation contributions depend on four different material parameters: C_{PSN}, A_{PSN}, C_{GB}, C_C. In order optimize the 6XXX recrystallization model to describe the behaviour of the investigated alloy, these constants are calculated by comparing the results of the experimental grain size analysis and the output of the numerical simulation.

The simulation was performed using Qform Extrusion FEM code, which is an Arbitrarian Lagrangian Eulerian software specifically optimized for the extrusion process. Optimized friction conditions between workpiece and tools are set within the code, and the parameters of the simulated materials can also be retrieved from a database (Table 3).

Table 3. Friction conditions [5].

Surface	Friction condition
Billet-Container	Sticking condition
Billet-Ram	Sticking condition
Billet-Die	Sticking condition
Bearings	Levanov model (m = 0.3, n = 1.25)

Table 4. AA6063 material parameters [5].

Material Properties	AA6063
Density [Kg/m3]	2690
Specific heat [J/kg K]	900
Thermal conductivity [W/m K]	200
Thermal expansivity [m/K]	2.34*10-5
Young's modulus [GPa]	68.9
Poisson's ratio	0.33

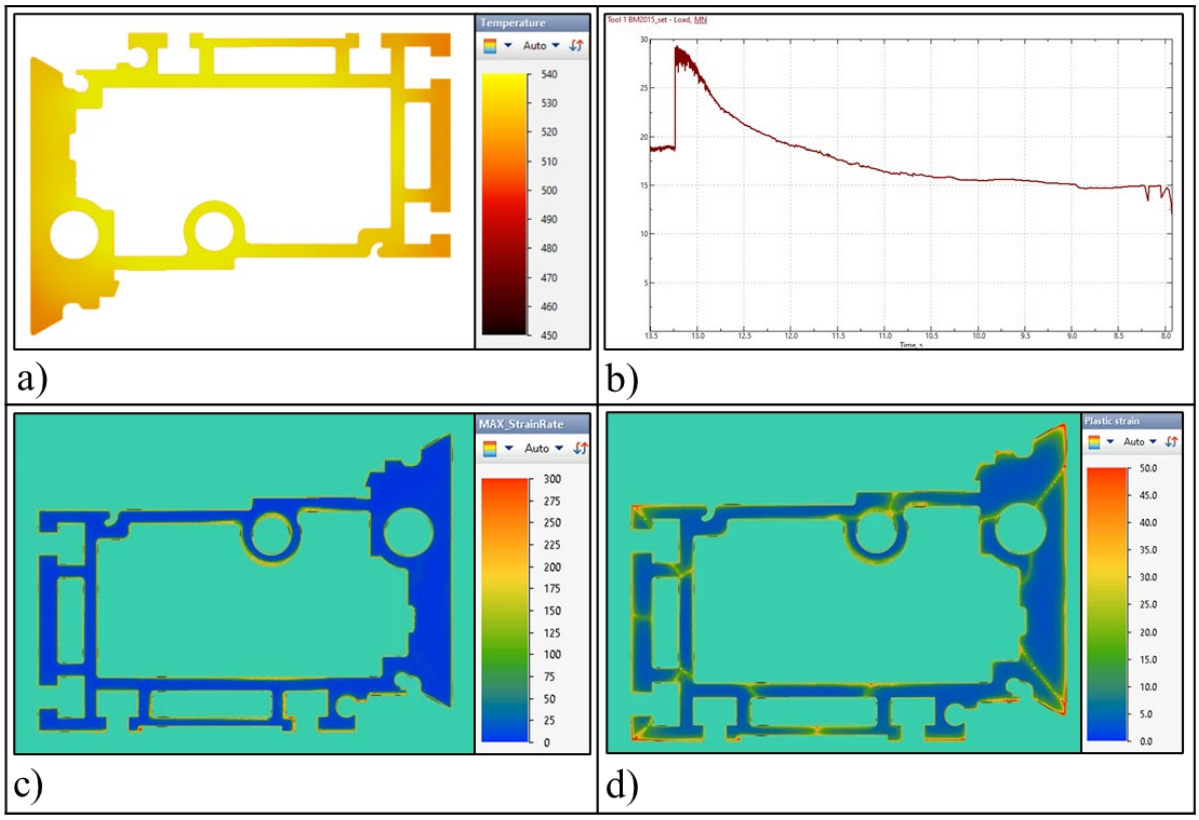

Fig. 2. Numerical simulation of a) temperature, b) extrusion load, c) maximum value of strain rate reached during the deformation, d) strain.

The accuracy of the simulation was verified by comparing the extrusion peak load and exit temperature acquired from the experiments and predicted with the finite element simulation. After the validation stage of the extrusion simulation, the values of strain, strain rate and temperature, taken in the 100 points selected for the grain size measurements (see "Experimental Investigation" chapter), were stored and 50 of these were used to calibrate the recrystallization model, therefore calculating the AA6063 model material constants. After the model completed and calibrated for the investigated alloy, it was implemented using a post-processing subroutine in Qform Extrusion. This integration allowed for efficient and accurate simulations of the microstructural evolution during the extrusion process, taking into account the material behavior at different stages of deformation and temperature conditions. Consequently, the FEM code performed a post-processing analysis to predict the grain size after the extrusion process, providing insights into the material microstructure evolution during the manufacturing process (Fig. 3).

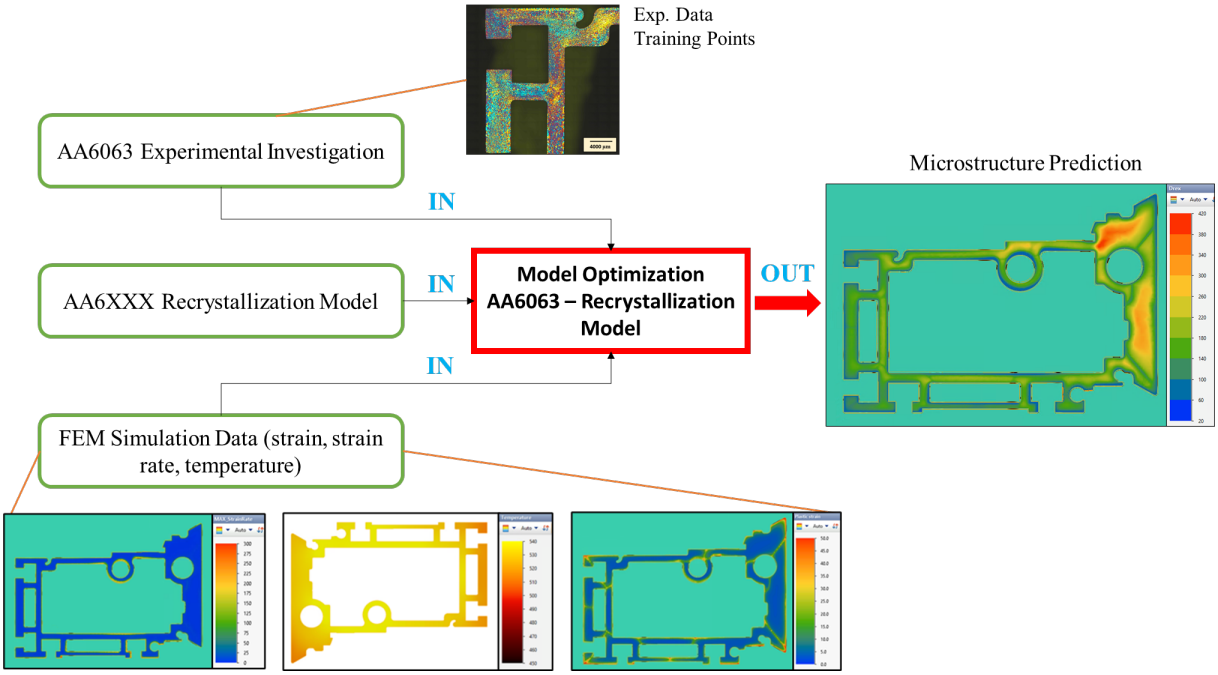

Fig. 3. Schematization of the methodology for the calibration of a AA6XXX recrystallization model for the prediction of the microstructure in the extrusion of a AA6063 aluminum alloy.

Results and Discussion

The recrystallization model's material constants were determined through the utilization of the Levenberg-Marquardt non-linear regression algorithm [5], implemented in Matlab®. To obtain these constants, the calibration set of points was utilized, where experimental grain size measurements were available. For each specific point in the calibration set, the Qform software was used for simulation, enabling the calculation of temperature, strain, and maximum strain rate values. Furthermore, a separate set of points known as the validation set was considered to assess and validate the accuracy of the numerical microstructure prediction results obtained through the calibration process. This approach ensured the robustness and reliability of the recrystallization model constants and the subsequent microstructure predictions. The calculated material constants are C_{PSN} = 4.99786 e13, A_{PSN} = 864698, C_{GB} = 0.00022381, C_C = 0.00022381.

In Fig. 4, the numerical simulation results depicting the grain size distribution after the complete static recrystallization (SRX) process are visually presented. The profile is color-coded, with red and blue regions denoting areas with relatively larger and smaller grain dimensions, respectively. The data revealed a range of grain size dimensions spanning from 43 µm to 418 µm.

Fig. 5 presents a comparative analysis between the experimentally measured grain sizes and their corresponding numerical predictions for the selected validation set of points. The x-axis represents the experimentally determined grain diameters, while the y-axis represents the dimensions predicted through numerical simulations. The alignment between the experimental and numerical data points along the 45° red line would indicate a high level of agreement between the two datasets, affirming the accuracy and reliability of the numerical model in predicting grain size evolution during the SRX process. To enhance the comprehension of prediction accuracy, two additional green lines were included, representing a ± 25% error range. Given the substantial influence of numerous process and metallurgical factors on the final grain size, as well as the complexity of the extruded geometries and the limitations associated with the chosen measurement methodology [10] for experimental grain dimension analysis, the ± 25% error range, which was similarly adopted by Donati L. et al. in [10], is regarded as indicative of good prediction accuracy.

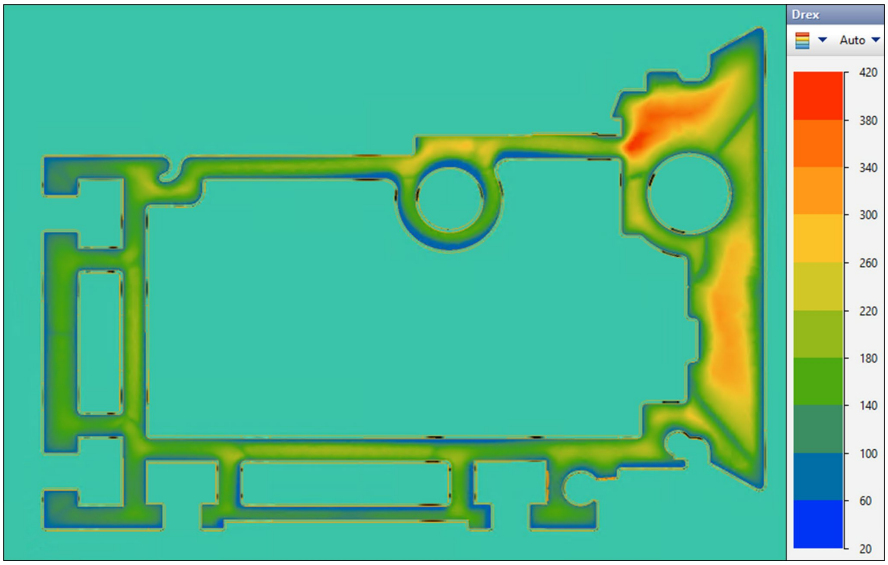

Fig. 4. Numerical prediction of the grain size after the SRX.

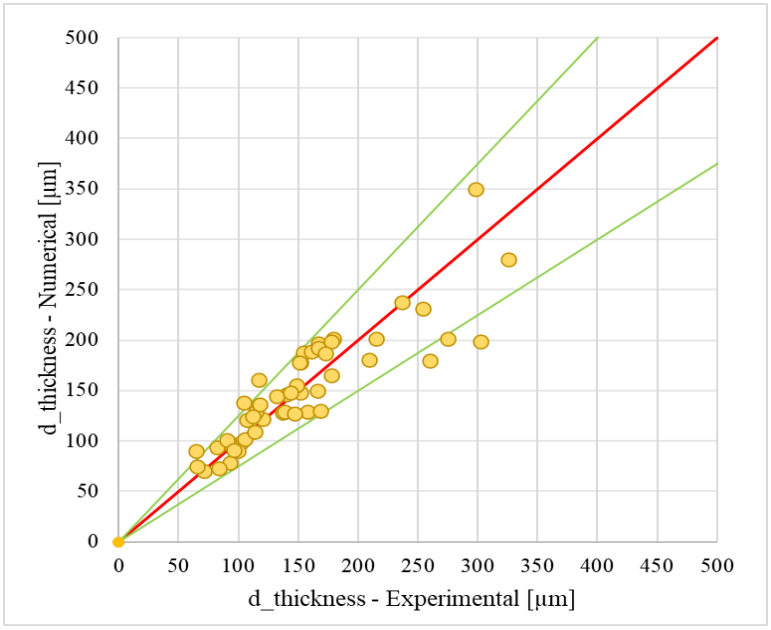

Fig. 5. Comparison between experimental and numerical grain size after SRX.

Conclusions

In this study, the 6XXX recrystallization model proposed by [8] was optimized for the AA6063 aluminum alloy, using the data of the finite element simulation performed with Qform Extrusion and the experimental grain size values collected from a AA6063 extruded hollow profile. Notably, the prediction error for the average grain size was found to remain below ±25% for over 90% of the analyzed points. This good level of agreement between experimental and numerical results demonstrates the reliability of the proposed model. The promising experimental-numerical concurrence must be further investigated by comparing the predictions with the experimental results of additional experimental campaign in order to assess the applicability for practical extrusion scenarios.

References

[1] L. Donati, B. Reggiani, R. Pelaccia, M. Negozio, S. Di Donato, Advancements in extrusion and drawing: a review of the contributes by the ESAFORM community, International Journal of Material Forming 15(6) (2022).

[2] R. Pelaccia, B. Reggiani, M. Negozio, L. Donati, Liquid nitrogen in the industrial practice of hot aluminium extrusion: experimental and numerical investigation, Interantional Journal of Advanced Manufacturing Technology 119(4) (2022) 1-15.

[3] R. Pelaccia, M. Negozio, L. Donati, B. Reggiani, L. Tomesani, Extrusion of Light and Ultralight Alloys with Liquid Nitrogen Conformal Cooled Dies: Process Analysis and Simulation, Journal of Materials Engineering and Performance 31(4) (2022) 1-11.

[4] M. Negozio, R. Pelaccia, L. Donati, B. Reggiani, T. Pinter, L. Tomesani, Finite Element Model Prediction of Charge Weld Behaviour in AA6082 and AA6063 Extruded Profiles, Journal of Materials Engineering and Performance 30 (2021) 4691-4699.

[5] M. Negozio, R. Pelaccia, L. Donati, B. Reggiani, Simulation of the microstructure evolution during the extrusion of two industrial-scale AA6063 profiles, Journal of Manufacturing Processes 99 (2023) 501-512.

[6] I. Kniazkin, R. Pelaccia, M. Negozio, S. Di Donato, L. Donati, B. Reggiani, N. Biba, R. Rezvykh, I. Kulakov, Investigation of the Skin Contamination Predictability by means of QForm UK Extrusion code, Materials Research Proceedings 28 (2023) 543-552.

[7] M. Negozio, R. Pelaccia, L. Donati, B. Reggiani, L. Tomesani, FEM validation of front-end and back-end defects evolution in a AA6063 and AA6082 aluminum alloys profiles, Procedia Manufacturing 47 (2020) 202-208.

[8] M. Negozio, R. Pelaccia, L. Donati, B. Reggiani, S. Di Donato, Experimental Analysis and Modeling of the Recrystallization Behaviour of a AA6060 Extruded Profile, Materials Research Proceedings 28 (2023) 477-486.

[9] A. Gamberoni, L. Donati, B. Reggiani, M. Haase, L. Tomesani, A. Tekkaya, Industrial Benchmark 2015: Process Monitoring and Analysis of Hollow EN AW-6063 Extruded Profile, Materials Today: Proceedings 2(10) (2015) 4714-4725.

[10] L. Donati, A. Segatori, M. El Mehtedi, L. Tomesani, Grain evolution analysis and experimental validation in the extrusion of 6XXX alloys by use of a lagrangian FE code, International Journal of Plasticity 46 (2013) 70-81.